Figure S1

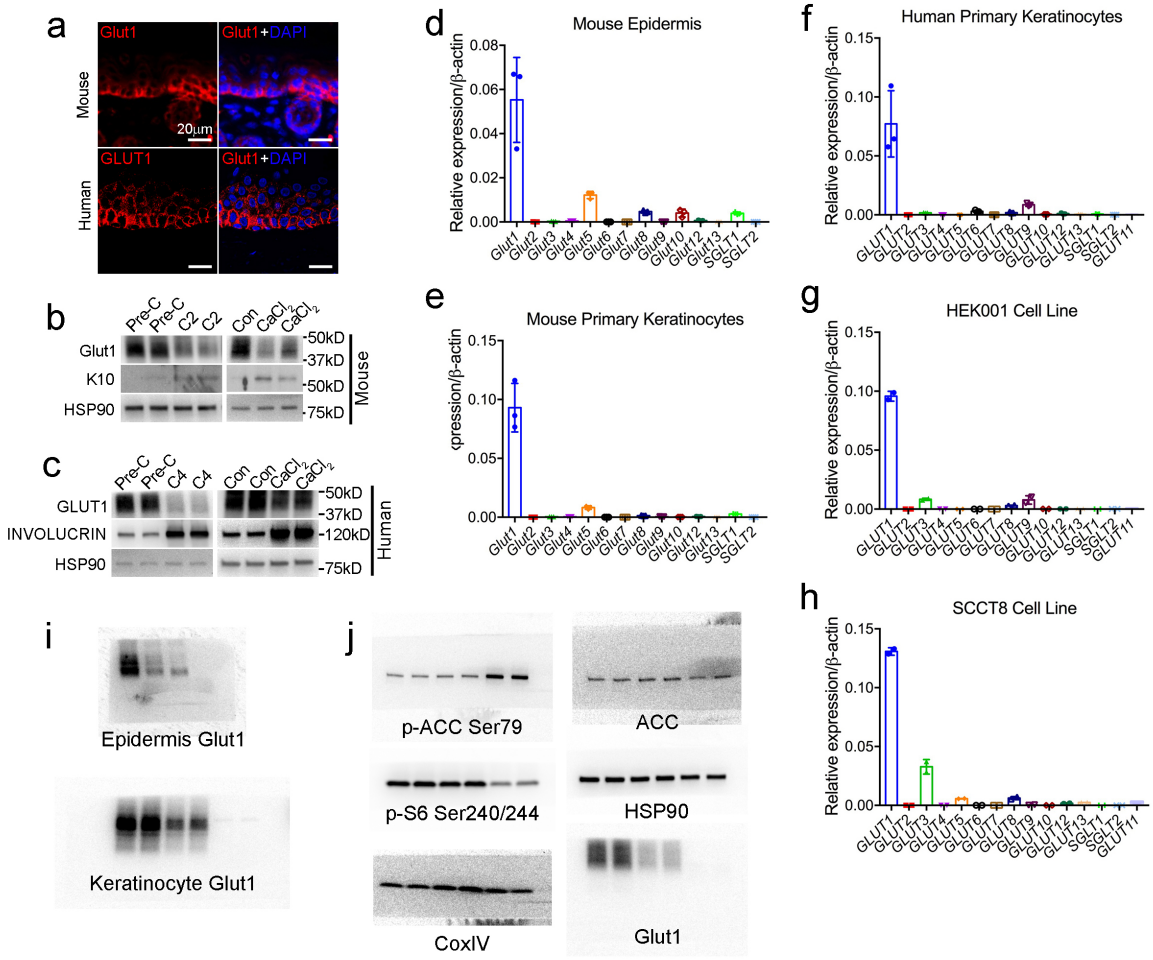

Figure S1. The expression pattern of *GLUT1* and additional *GLUT/SGLT* transporters. **(a)** Immunostaining of Glut1 in 2-month-old mouse dorsal skin and adult human abdominal skin showing expected expression in basal keratinocytes. Similar results obtained in 2 independent experiments. **(b, c)** Glut1, K10 (Keratin10) or INVOLUCRIN abundance in primary cultured mouse (b) or human (c) keratinocytes before confluence (Pre-C), 2 or 4 days after confluence (C2 or C4), or treated with 1 mM $CaCl_2$ for 2 days. Similar results obtained in 3 independent experiments. **(d-h)** The mean expression of *Glut* family members in epidermis from 1-week-old mice (d) (n=3 independent mice), primary cultured keratinocytes from 1-week-old mice (e) (n=3 independent mice), primary cultured keratinocytes from adult human abdomen skin (f) (n=3 independent preparations), an immortalized human keratinocyte cell line HEK001 (g)) (n=2 preparations), and SCCT8 a human squamous cell carcinoma cell lines (h) (n=2 preparations). Uncropped gels from Fig. 1a **(j)** and 1h **(j)**.

Figure S2

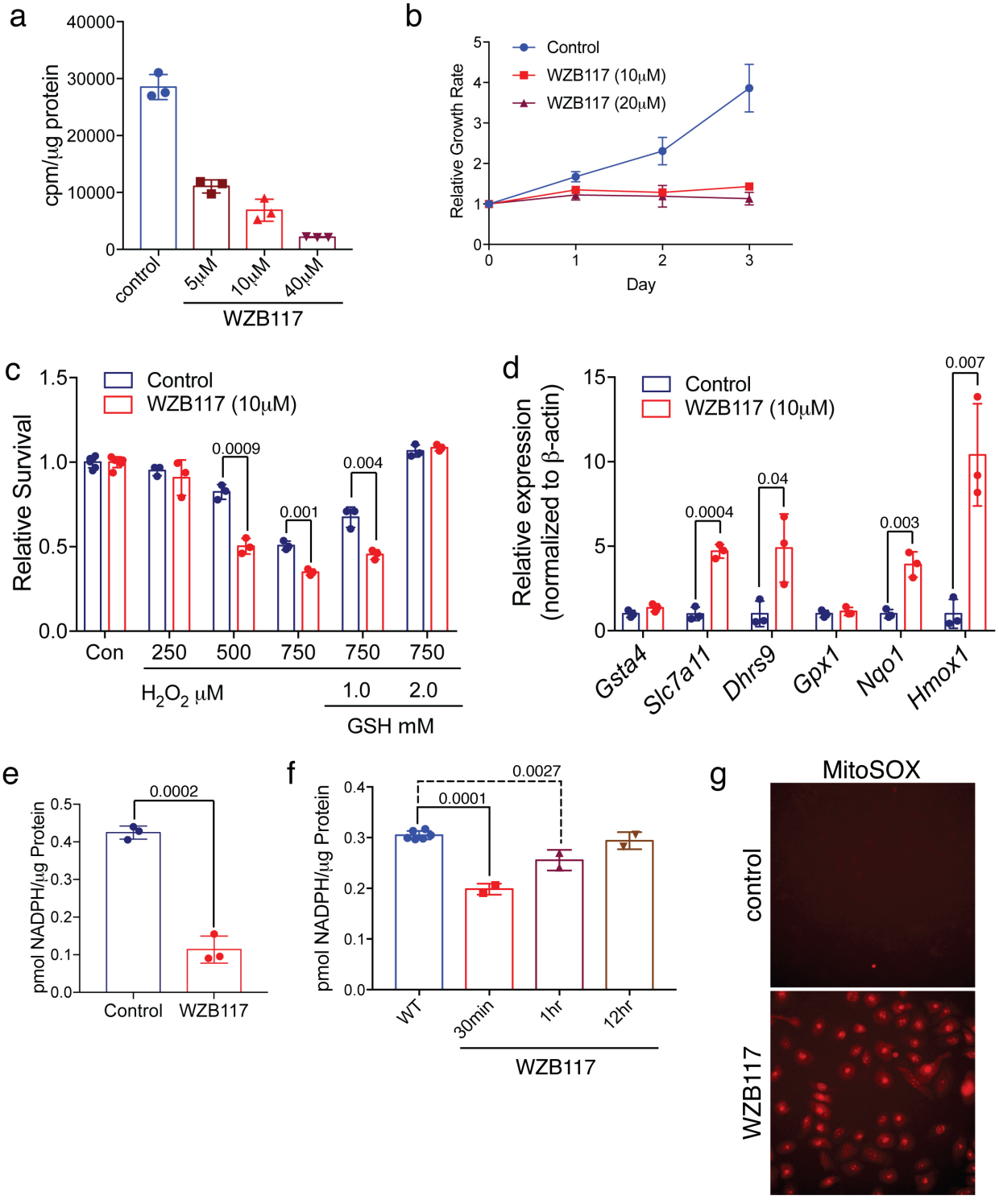
a
cpm/μg protein
40000
30000
20000
10000
0
control
5μM
10μM
40μM
WZB117
b
Relative Growth Rate
Control
WZB117 (10μM)
WZB117 (20μM)
Day
c
Relative Survival
Control
WZB117 (10μM)
0.0009
0.001
0.004
Con
250
500
750
750
750
H2O2 μM
1.0
2.0
GSH mM
d
Relative expression
(normalized to β-actin)
Control
WZB117 (10μM)
0.0004
0.04
0.003
0.007
Gsta4
Slc7a11
Dhrs9
Gpx1
Nqo1
Hmox1
e
pmol NADPH/μg Protein
0.0002
Control
WZB117
f
pmol NADPH/μg Protein
0.0027
0.0001
WT
30min
1hr
12hr
WZB117
g
MitoSOX
control
WZB117

Figure S2. Acute chemical inhibition of GLUT1 impairs proliferation and redox homeostasis in primary human and mouse keratinocytes.
(a) Uptake of 2-deoxy-D-glucose (2-DG) in primary human keratinocytes after treatment with increasing doses of WZB-117 or DMSO control (n=3 independent cultures). *P*=0.0001 for all WZB117 concentrations compared to control. **(b)** The growth rate of primary human keratinocytes as assessed by cell number at the indicated time point. Equal numbers of cells were seeded in triplicate on day 0. Similar results obtained in 3 independent experiments. **(c)** Primary human keratinocytes were treated with H_2O_2 with or without GSH and cell number was assessed after 24 hours. The surviving fraction was calculated relative to untreated cells of the same group (n=3 independent cultures). **(d)** RT-PCR for redox homeostasis genes; *Scl7a11*, *Dhrs9*, *Nqo1,* and *Hmox1* show significant upregulation after treatment of primary human keratinocytes with WZB117 (n=3 independent preparation). **(e)** Mean levels of NADPH in primary human keratinocytes with or without WZB117 (10μM for 30 min) (n=3 independent cultures). **(f)** Primary mouse keratinocytes (WT) were treated with WZB117 (10μM) for the indicated times and NADPH levels measured (n=2 mice). **(g)** MitoSOX staining of primary human keratinocytes demonstrates increased mitochondrial ROS in primary keratinocytes after acute treatment with WZB117 (10μM for 30 min). Similar results obtained in 3 independent experiments. Data are presented as mean±s.d. *P* values (indicated about relevant comparison) were calculated by one-way ANOVA with Dunnett test (a, f) or two-tailed t-test (c-e).

Figure S3

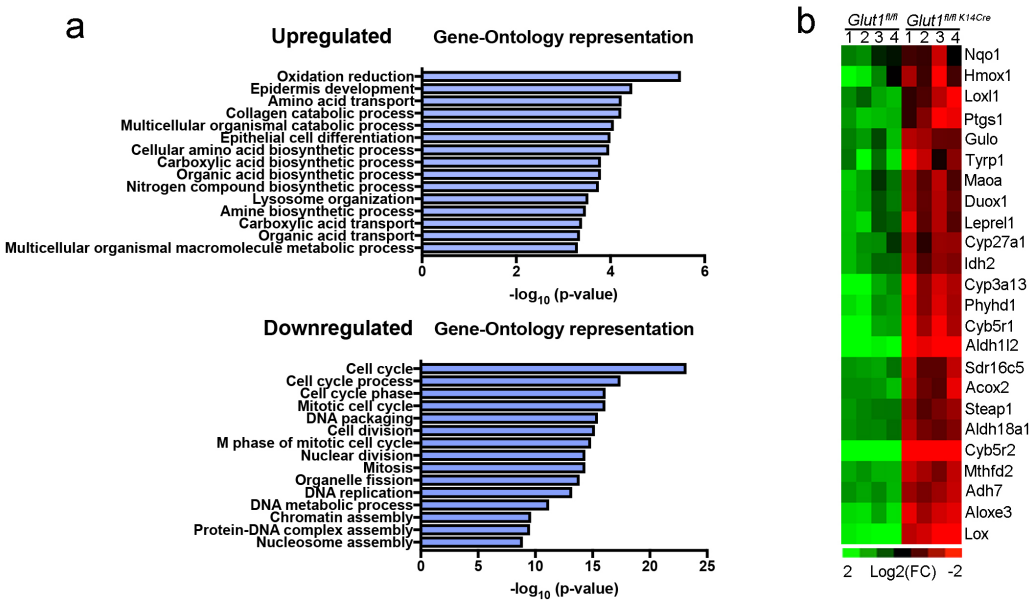

Figure S3. Effects of Glut1 deletion on gene expression.
(a) RNA from *WT* and *K14.Glut1* keratinocytes (n=8 mice per genotype) was used to probe an Affymetrix GeneChip Mouse Gene 2.0 ST Array. Gene ontology analysis of pathways upregulated (top) and downregulated (bottom) more than two fold in *K14.Glut1* keratinocytes. **(b)** Heat map of oxidative stress related genes that increased more than two fold in *K14.Glut1* keratinocytes. See also Fig. 2b.

Figure S4

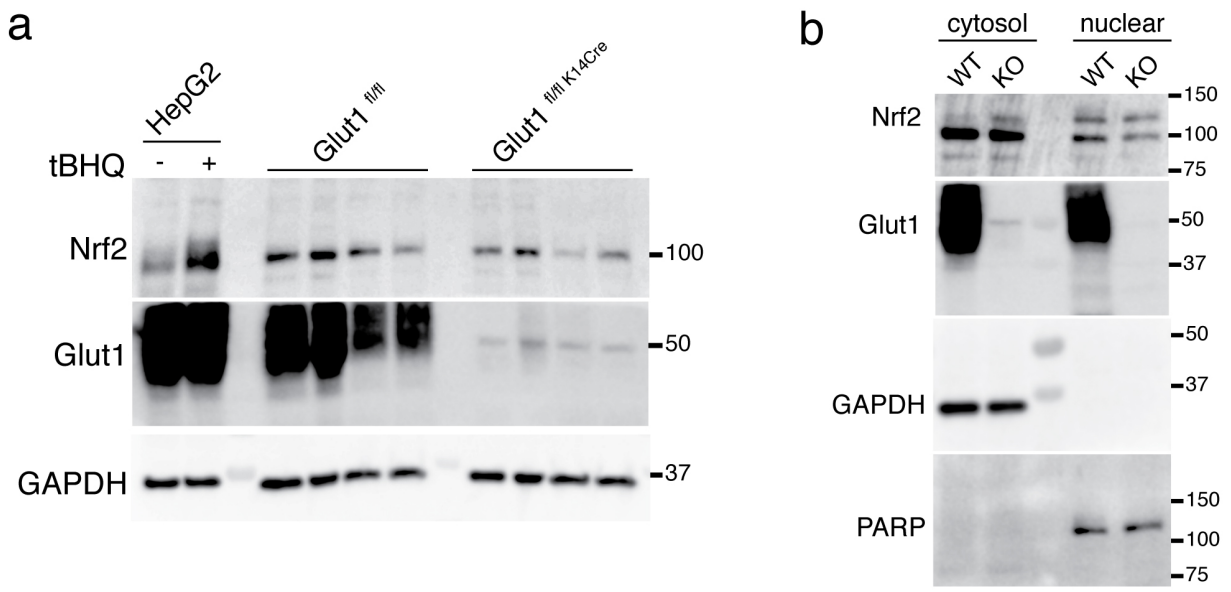

Figure S4. The effect of *Glut1* deletion on Nrf2.
(a) *K14.Glut1* (n=4) primary keratinocytes do not show increased levels of Nrf2 compared to *WT* littermates. *Tert*-Butylhydroquinone (t-BHQ) is a positive control for Nrf2 induction. **(b)** Fractionation of primary keratinocytes reveals no increase in nuclear Nrf2 after *Glut* deletion. Similar results obtained in 3 independent experiments.

Figure S5

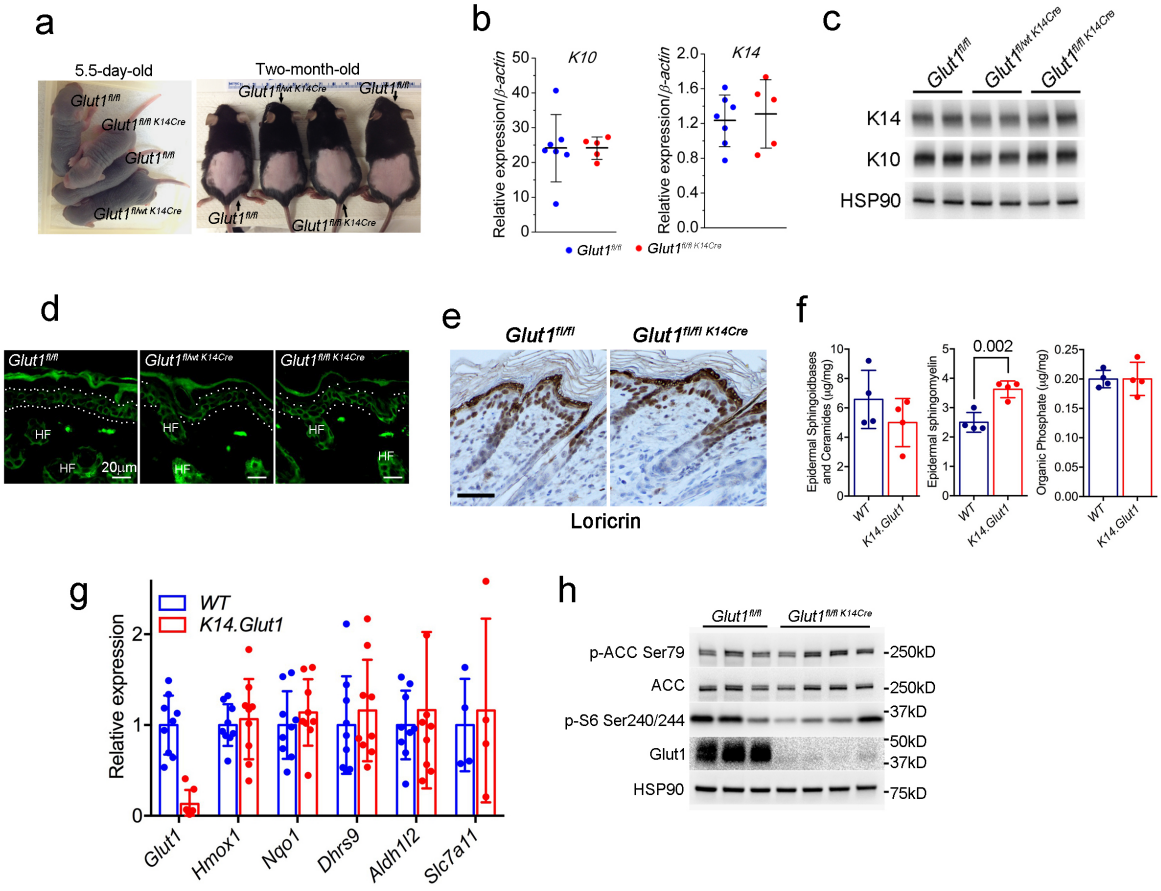

Figure S5. *K14.Glut1* mice show no defects in skin development and homeostasis. (a) Photos of 5.5 day old and depilated dorsal skin of 2 month *WT*, K14.*Glut1*$^{fl/wt}$, and *K14.Glut1* mice reveal no discernible differences between the littermates. Similar results obtained in 3 independent experiments. **(b)** K10 (Keratin10) and K14 mRNA levels in harvested epidermis of one-week-old WT (n=7) and K14.Glut1 (n=5) mice. **(c)** K10 and K14 protein expression in the epidermis of one-week-old mice. Similar results obtained in 5 independent animals. **(d)** K14 immunofluorescence of the dorsal skin of one-week-old mice revealed no differences in the expression pattern of K14. Dotted lines indicate the dermoepidermal junction. Similar results obtained in 2 independent experiments. **(e)** Staining for loricin, a terminal differentiation marker, reveals no differences between *WT* and *K14.Glut1* mice. Similar results obtained in 2 independent experiments. **(f)** Lipids were isolated from the epidermis of 5-day-old mice and analyzed by LC-MS/MS. Total epidermal sphingoidbases and ceramides, sphingomyelins, and organic phosphate (which indirectly reflect phospholipid levels) (n=4 each genotype). Sphingomyelin levels are significantly elevated in K14.Glut1 epidermis. **(g)** RT-PCR for redox homeostasis genes from the epidermis of one week old *WT* and *K14.Glut1* (n=4 mice each group) mice show no significant differences without stressors. **(h)** WB from the epidermis of one week old mice suggest no differences in the indicated proteins. Similar results obtained in 3 independent experiments. Data presented as mean± s.d. *P* values (indicated about relevant comparison) were calculated by two-tailed t-test (f).

Figure S6

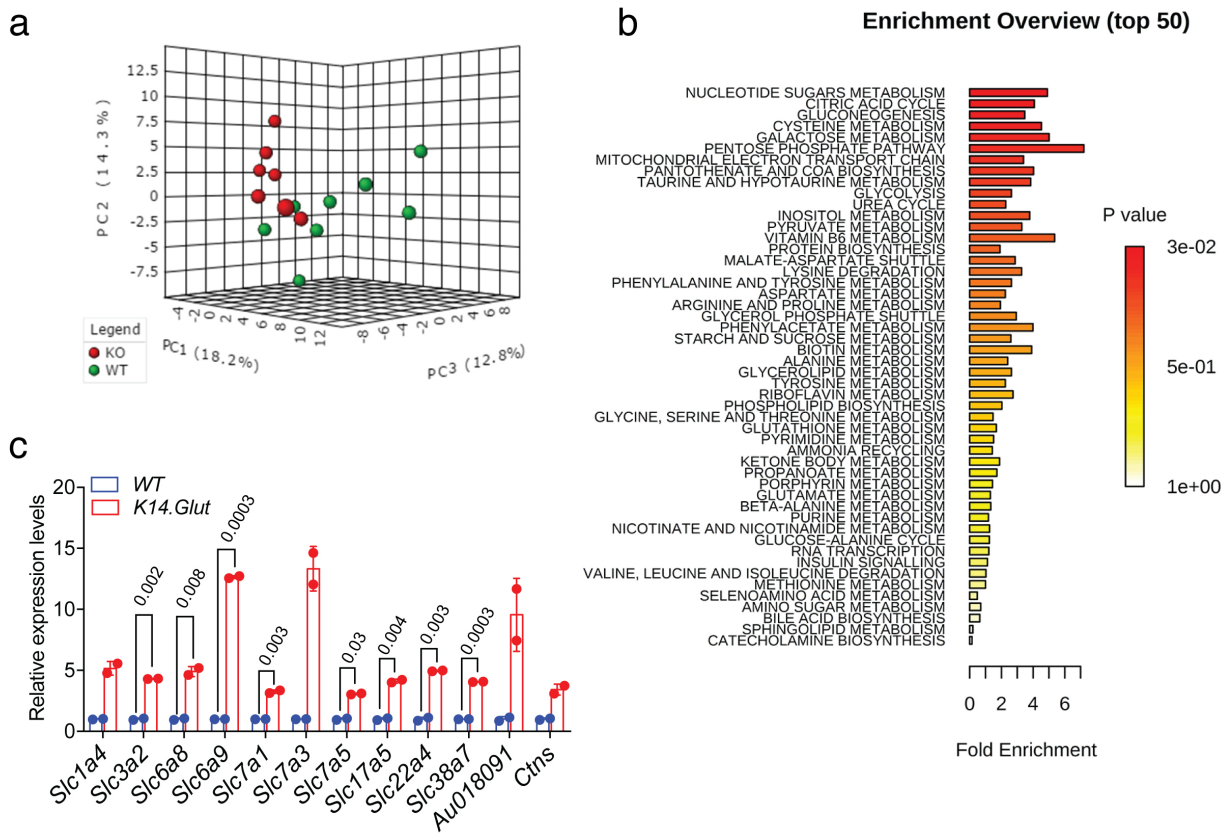

Figure S6. Metabolic reprogramming in *K14.Glut1* mice.
(a) Principal component analysis of the metabolites from epidermis obtained from *WT* and *K14.Glut1* mice (n=8 each) reveal distinct clustering of the genotypes. **(b)** Quantitative enrichment analysis of the metabolites from epidermis obtained from *WT* and *K14.Glut1* mice mice using the MetaboAnalyst 3.0 software. (n=8 mice per genotype) **(c)** RT-PCR analysis of amino acid and carboxylic acid transporter genes from *K14.Glut1* keratinocytes show significant upregulation of multiple transporters in *K14.Glut1* mice compared to *WT* animals. Data presented as mean± s.d. *Q* values (indicated about relevant comparison) were calculated by two-tailed t-test with adjustment for the False Discovery Rate.

Figure S7

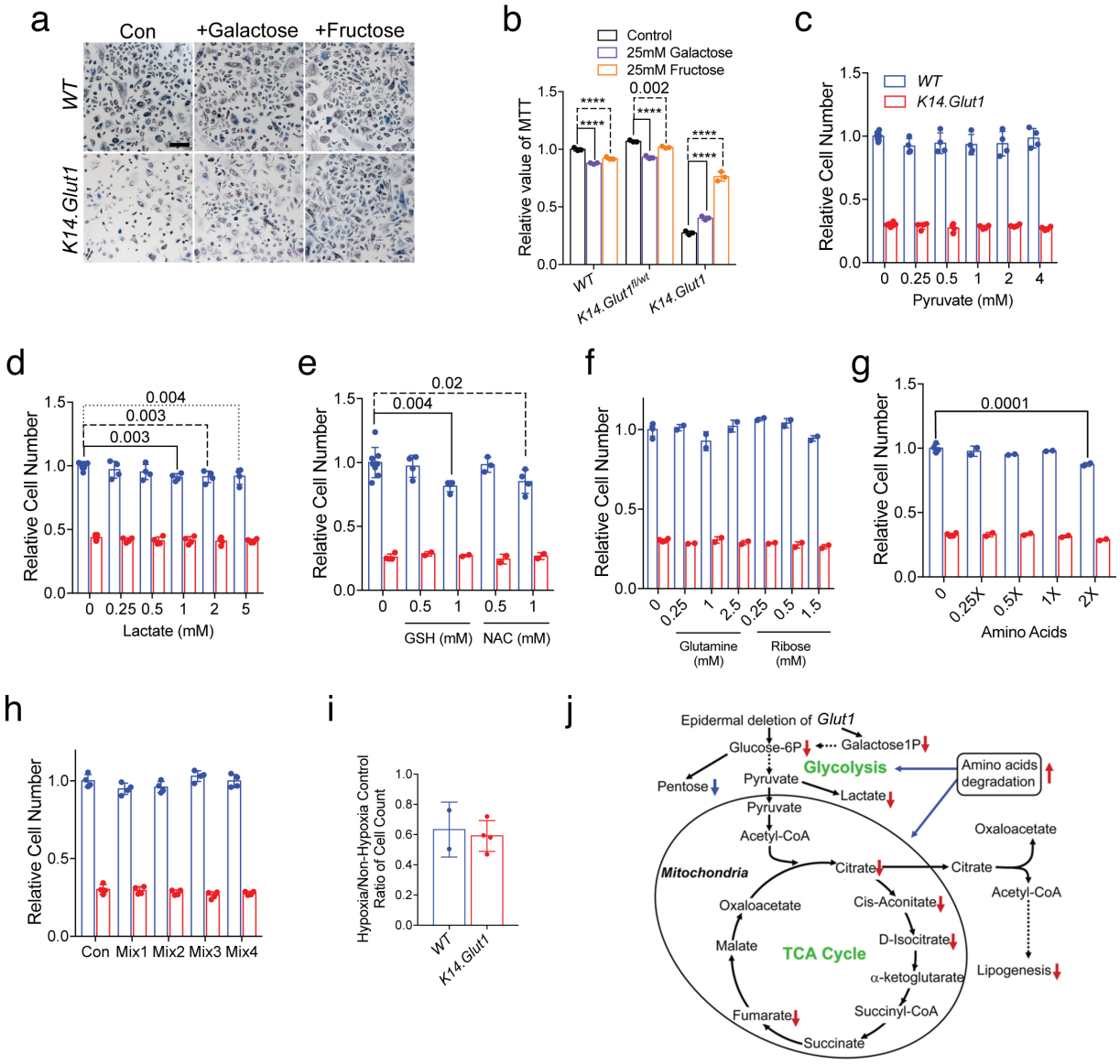
a
Con
+Galactose
+Fructose
WT
K14.Glut1
b
Control
25mM Galactose
25mM Fructose
Relative value of MTT
0.002
****
WT
K14.Glut1fl/wt
K14.Glut1
c
WT
K14.Glut1
Relative Cell Number
Pyruvate (mM)
d
Relative Cell Number
0.004
0.003
0.003
Lactate (mM)
e
Relative Cell Number
0.02
0.004
GSH (mM)
NAC (mM)
f
Relative Cell Number
Glutamine (mM)
Ribose (mM)
g
Relative Cell Number
0.0001
Amino Acids
h
Relative Cell Number
Con Mix1 Mix2 Mix3 Mix4
i
Hypoxia/Non-Hypoxia Control Ratio of Cell Count
WT
K14.Glut1
j
Epidermal deletion of Glut1
Glucose-6P
Galactose1P
Glycolysis
Amino acids degradation
Pentose
Pyruvate
Lactate
Acetyl-CoA
Oxaloacetate
Mitochondria
Citrate
Cis-Aconitate
D-Isocitrate
α-ketoglutarate
Succinyl-CoA
Succinate
Fumarate
Malate
TCA Cycle
Lipogenesis

Figure S7. Partial rescue of *Glut1* deficiency by fructose, galactose, and fatty acids, but not other metabolites.

(a) *WT* and *K14.Glut1* keratinocytes obtained from one-week-old mice were cultured in complete KSFM medium, or complete KSFM medium supplemented with 25mM galactose or 25mM fructose for 36 hours, then they were incubated with 0.5 mg/ml MTT, pictures were taken after 2 hours of incubation. Similar results obtained in 2 independent experiments. **(b)** 25 mM Galactose or 25 mM Fructose were supplemented in the indicated genotype; cell proliferation was assessed by MTT assay after 36 hours (n=3 mice per genotype). **(c-h)** *WT* and *K14.Glut1* keratinocytes obtained from one-week-old mice were cultured in complete KSFM medium, or complete KSFM medium supplemented different concentrations of **(c)** pyruvate (n=4 mice per genotype), **(d)** lactate (n=4 mice per genotype), **(e)** Glutathione (GSH), N-Acetyl Cysteine (NAC) (n=2 mice per genotype), **(f)** glutamine or ribose (n=2 mice per genotype), **(g)** RPMI 1640 amino acids solution (n=2 mice per genotype), or **(h**) mixtures of these supplements (Mix1: 1mM Glutamine, 0.5mM Pyruvate, 0.5X AA, 0.5mM Ribose, 0.125mM GSH; Mix2: 2mM Glutamine, 1mM Pyruvate, 1X AA, 1mM Ribose, 0.25mM GSH. Mix3: 0.5X AA, 0.5mM Ribose, 0.25mM GSH. Mix4: 0.5X AA, 0.5mM Ribose) (n=4 mice per genotype). Cell number scored after 36 hours of growth. **(i)** Growth in hypoxic conditions did not rescue K14.Glut1 keratinocyte growth after culturing for 48 hours (n=2 mice per genotype). (error bars=SD. *P<0.05, **P<0.01; two tailed student's t-test). Bars show mean$\pm$s.d. *P* values (indicated about relevant comparison, ****P<0.0001) were calculated by two-way ANOVA with Holm-Sidak tests (c-h) or two-tailed t-test (i).

Figure S8

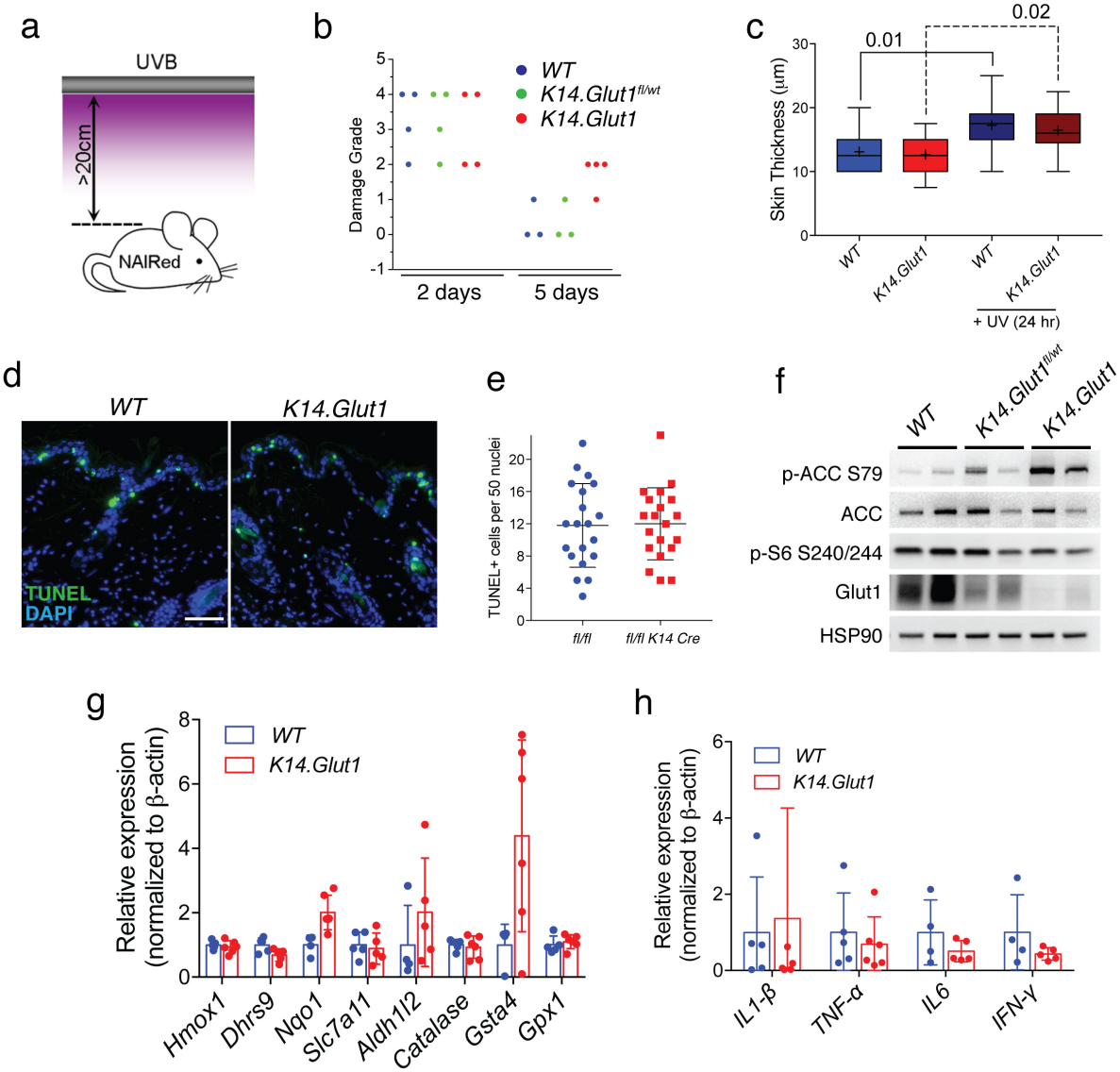
a
UVB
>20cm
NAIRed
b
WT
K14.Glut1fl/wt
K14.Glut1
Damage Grade
2 days
5 days
c
0.01
0.02
Skin Thickness (μm)
WT
K14.Glut1
WT
K14.Glut1
+ UV (24 hr)
d
WT
K14.Glut1
TUNEL
DAPI
e
TUNEL+ cells per 50 nuclei
fl/fl
fl/fl K14 Cre
f
WT
K14.Glut1fl/wt
K14.Glut1
p-ACC S79
ACC
p-S6 S240/244
Glut1
HSP90
g
WT
K14.Glut1
Relative expression (normalized to β-actin)
Hmox1
Dhrs9
Nqo1
Slc7a11
Aldh1l2
Catalase
Gsta4
Gpx1
h
WT
K14.Glut1
Relative expression (normalized to β-actin)
IL1-β
TNF-α
IL6
IFN-γ

Figure S8. *K14.Glut1* mice have an impaired response to UVB irradiation.
(a) Schematic for UVB irradiation. **(b)** The damage grade (GVHD scale) was assessed by a blinded dermatopathologist 2 or 5 days after 50 mJ/cm^2 UVB irradiation in the indicated genotype (n=3 each group) mice. **(c)** Epidermal thickness was measured with a calibrated ocular micrometer. *WT* and *K14.Glut1* skin shows no significant differences before or 24 hours after UVB. Both genotypes show significant thickening after UVB irradiation (n=4 mice per genotype with multiple independent sections per mouse). **(d)** *WT* and *K14.Glut1* skin was harvested 24 hours after UVB irradiated and assessed by TUNEL (Thermo Fisher) assay. Similar results obtained in 4 separate animals. **(e)** The number of TUNEL positive nuclei (per 50 nuclei) were scored; there were no significant differences in apoptosis between *WT* and *K14.Glut1* skin after UVB irradiation (n=4 mice per genotype with multiple independent sections per mouse). **(f)** Western Blot analysis of the abundance of p-ACC Ser79, ACC, p-S6 Ser240/244, Glut1 in epidermis obtained from 2-month-old mice of the indicated genotype. *K14.Glut1* mice show increased p-ACC and decreased p-S6 consistent with growth inhibition. Similar results obtained in 5 independent animals. **(g)** RT-PCR for redox homeostasis genes from the epidermis of one week old *WT* and *K14.Glut1* (n=4 mice each group) mice 24 hours after UVB irradiation. **(h)** RT-PCR for inflammatory cytokines from the epidermis of one week old *WT* and *K14.Glut1* (n=4 mice each group) mice 24 hours after UVB irradiation. Box shows 25th-75th percentiles, whiskers show min to max, crosses show means, and lines show medians. Bars show mean$\pm$s.d. *P* values (indicated about relevant comparison) were calculated by one way ANOVA with Holm-Sidak tests (c).

Figure S9

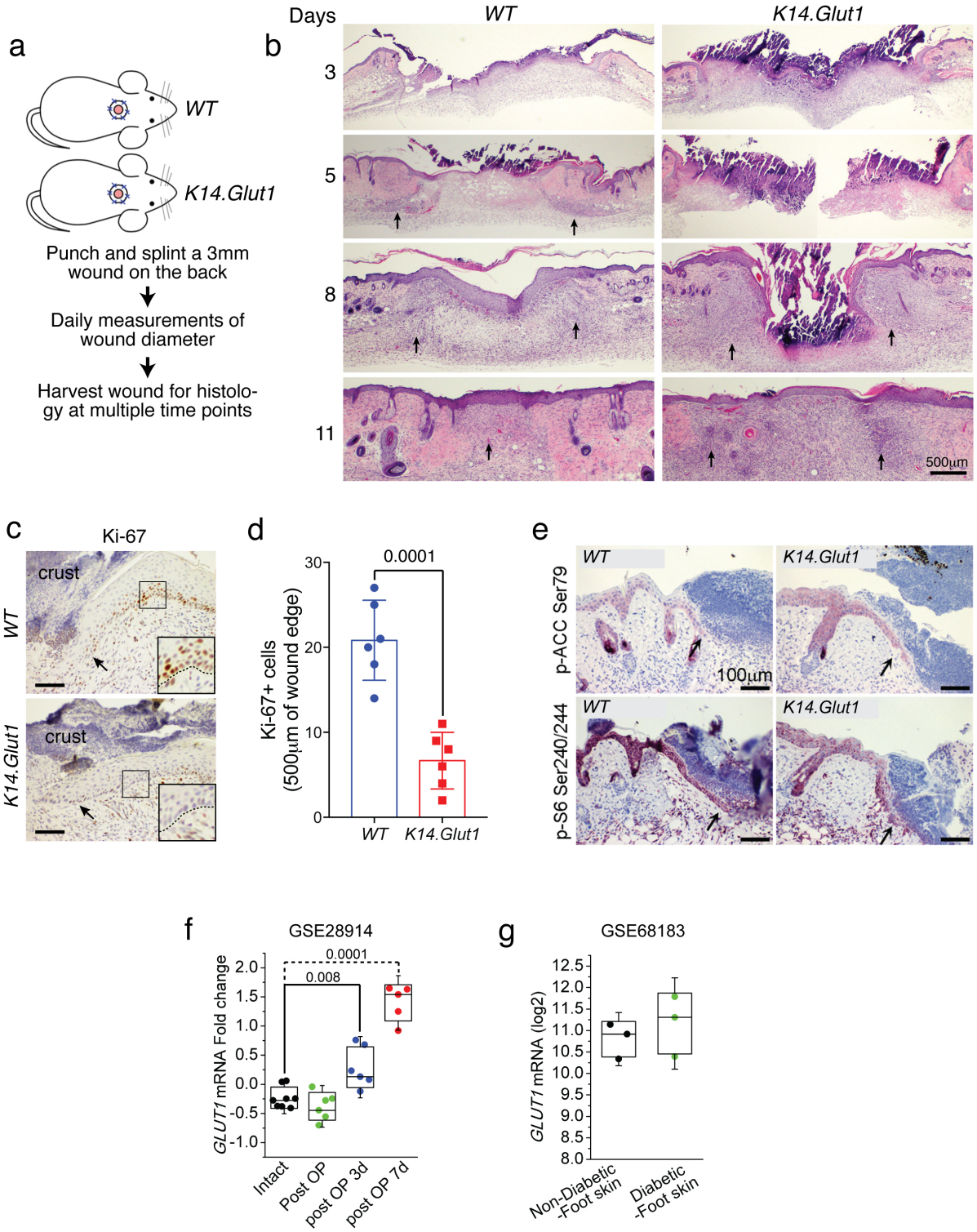
a
WT
K14.Glut1
Punch and splint a 3mm wound on the back
Daily measurements of wound diameter
Harvest wound for histology at multiple time points
b
Days
WT
K14.Glut1
3
5
8
11
500μm
c
Ki-67
WT
K14.Glut1
crust
crust
d
0.0001
Ki-67+ cells (500μm of wound edge)
30
20
10
0
WT
K14.Glut1
e
WT
K14.Glut1
p-ACC Ser79
p-S6 Ser240/244
100μm
f
GSE28914
0.0001
0.008
GLUT1 mRNA Fold change
2.0
1.5
1.0
0.5
0.0
-0.5
-1.0
Intact
Post OP
post OP 3d
post OP 7d
g
GSE68183
GLUT1 mRNA (log2)
12.5
12.0
11.5
11.0
10.5
10.0
9.5
9.0
8.5
8.0
Non-Diabetic -Foot skin
Diabetic -Foot skin

Figure S9. *K14.Glut1* mice show impaired wound healing *in vivo* and *in vitro*.
(a) Schematic for punch excision and wound splinting model. **(b)** A time course of wound repair reveals that *K14.Glut1* mice show delayed wound healing relative compared to *WT* littermates. Both genotypes show dense lymphohistiocytic infiltrates (arrows) during the wound healing time course. Similar results obtained in 3 independent animals. **(c)** Ki-67 immunostaining reveals decreased proliferation in K14.Glut1 mice 5.5 days after wounding. Dotted line in inset indicated the dermo-epidermal junction. Similar results obtained in 3 independent animals. **(d)** Quantitation of Ki-67 positive keratinocytes within 500μm of the wound edge in WT and *K14.Glut1* mouse skin. (n=3 independent mice with 2 independent wound sections) **(e)** Immunohistochemistry reveals p-ACC Ser79, and p-S6 Ser240/244 in wounding skin from WT and K14.Glut1 mice harvested 3 days after wounding. Arrow indicates the edge of a wound. Similar results obtained in 3 independent animals. **(f)** Serial biopsies from the wound edge of healthy volunteers (GSE28914) revealed significant increases in *GLUT1* expression 3d and 7d after wounding (n=6 individuals). **(g)** Biopsies from the foot skin of normal and diabetic skin (GSE68183) revealed no significant differences in *GLUT1* expression between normal and diabetic foot skin (n=3 individuals). Box shows 25^{th}-75^{th} percentiles, whiskers 1^{st}-99^{th} percentiles, and lines show medians. Bars show mean±s.d. *P* values (indicated about relevant comparison) were calculated by two-tailed t-test (d) or one-way ANOVA with Holm-Sidak tests (f).

Figure S10

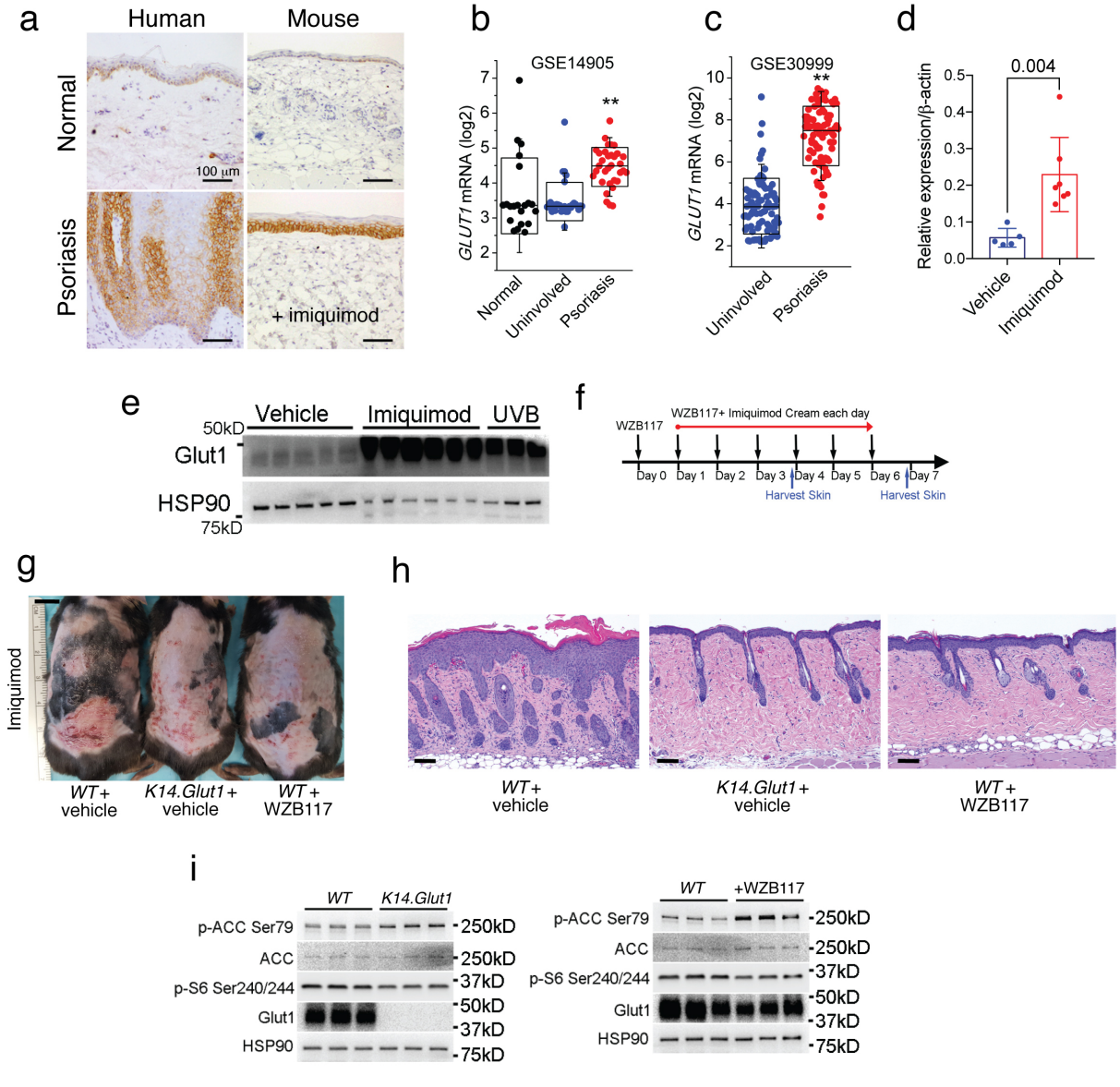
a
Human
Mouse
Normal
Psoriasis
100 μm
+ imiquimod
b
GSE14905
GLUT1 mRNA (log2)
**
Normal
Uninvolved
Psoriasis
c
GSE30999
GLUT1 mRNA (log2)
**
Uninvolved
Psoriasis
d
0.004
Relative expression/β-actin
Vehicle
Imiquimod
e
Vehicle
Imiquimod
UVB
50kD
Glut1
HSP90
75kD
f
WZB117
WZB117+ Imiquimod Cream each day
Day 0
Day 1
Day 2
Day 3
Day 4
Day 5
Day 6
Day 7
Harvest Skin
Harvest Skin
g
Imiquimod
WT+ vehicle
K14.Glut1+ vehicle
WT+ WZB117
h
WT+ vehicle
K14.Glut1+ vehicle
WT+ WZB117
i
WT
K14.Glut1
p-ACC Ser79
ACC
p-S6 Ser240/244
Glut1
HSP90
250kD
250kD
37kD
50kD
37kD
75kD
WT
+WZB117
p-ACC Ser79
ACC
p-S6 Ser240/244
Glut1
HSP90
250kD
250kD
37kD
50kD
37kD
75kD

Figure S10. Chemical or genetic inhibition of Glut1 rescues psoriasiform dermatitis. (a) Immunohistochemistry reveals Glut1 overexpression in lesional skin from psoriasis patients and after application of imiquimod to the dorsal skin of mice. Representative of 3 independent experiments. **(b)** *GLUT1* levels, as derived from the indicated GSE dataset, in active psoriasis lesions compared to normal skin and uninvolved skin. **(c)** *GLUT1* levels, as derived from the indicated GSE dataset, in active psoriasis lesions compared to uninvolved skin. **(d)** GLUT1 mRNA is significantly overexpressed in mouse skin after imiquimod treatment (n=5 mice per group). **(e)** GLUT1 protein is overexpressed in mouse skin after imiquimod treatment or UVB irradiation. Similar results obtained in 2 independent experiments. **(f)** Timeline of Glut1 inhibitor WZB117 and imiquimod applications. **(g)** Photos of skin in *WT*, *K14.Glut1*, and WZB117 treated *WT* mice treated with imiquimod. *K14.Glut1* and WZB117 treated mice show decreased, scale, erythema, and thickening after 6 days of imiquimod treatment. Similar results obtained in 3 independent experiments (Bar=1cm). **(h)** Histology from back skin of mice treated with imiquimod as inidicated. Similar results obtained in 3 independent experiments. **(i)** WB analysis of the expression of p-ACC Ser79, ACC, p-S6 Ser240/244, Glut1 in the skin of *WT* and *K14.Glut1* or *WT* and WZB117 treated *WT* in epidermis three days after imiquimod treatment. Similar results obtained in 2 independent experiments. Box shows 25^{th}-75^{th} percentiles, whiskers 1^{st}-99^{th} percentiles, and lines show medians. Bars show mean ± s.d. *P* values (as indicated, **P<0.001) were calculated by two-tailed t-test (b-d).

Figure S11

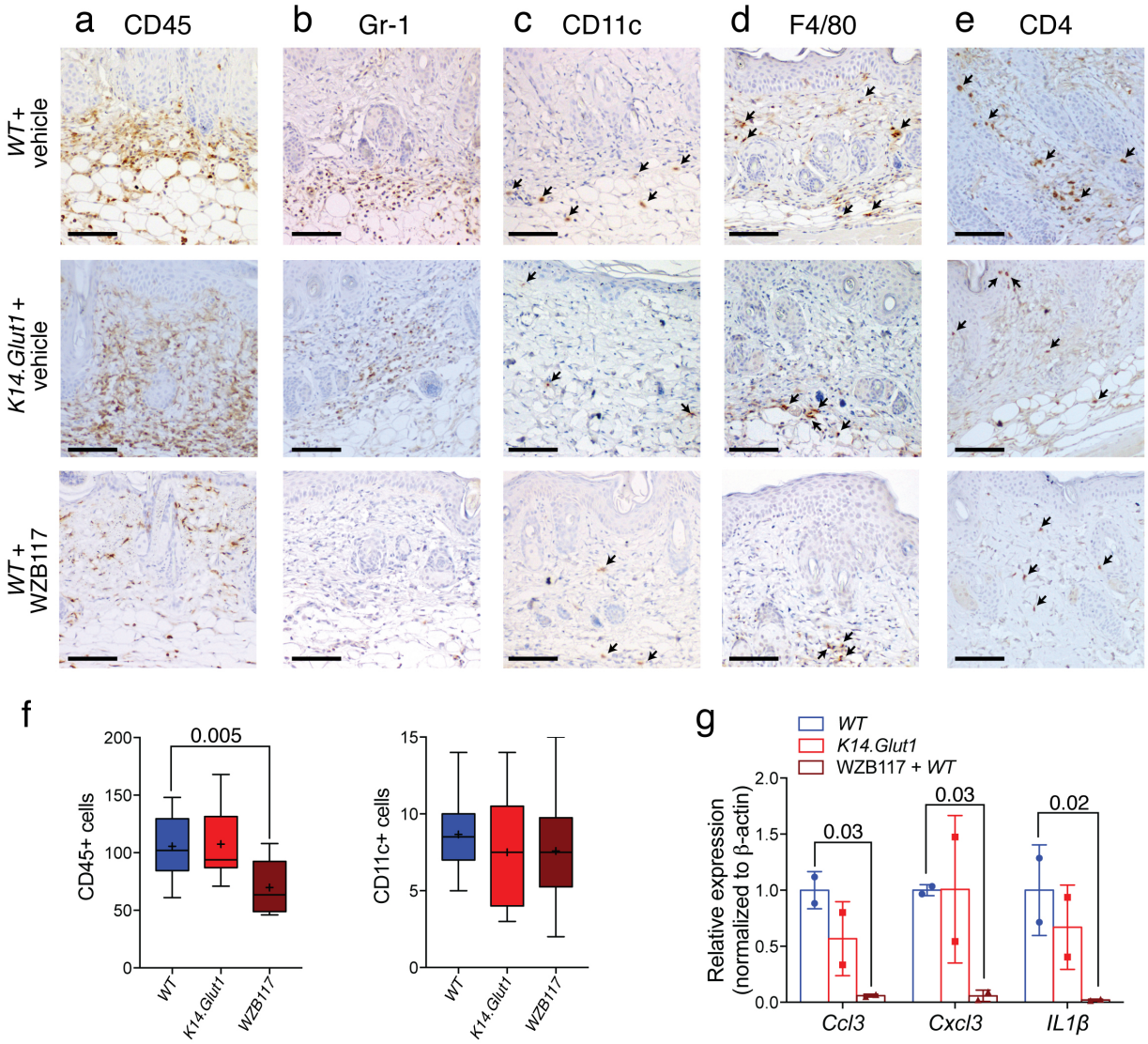

Figure S11. Inflammation associated with imiquimod-induced psoriasis-like dermatitis is rescued by chemical inhibition of glucose transport.
(a-e) Representative images of CD45, Gr-1, CD11c, F4/80, and CD4 cells in *WT*, *K14.Glut1*, or WZB117 treated mice. Treatment with WZB117 significantly decreases the number of induced by imiquimod. Arrows indicate a subset of positively staining cells. Similar results obtained in 3 indendently treated mice (Bar=100 μm). **(f)** Quantification of cells stained for the indicated marker in *WT*, *K14.Glut1*, or WZB117 treated mice (n=4 mice per group). **(g)** Expression of cytokines (Ccl3, Cxcl3, IL-1b) as assessed by qRT-PCR from the skin of mice *WT*, *K14.Glut1*, or WZB117-treated *WT* mice psoriasis after treatment with imiquimod (n=2 mice per group). Box shows 25th-75th percentiles, whiskers show min to max, crosses show means, and lines show medians. Bars show mean±s.d.. *P* values (indicated about relevant comparison) were calculated by one-way ANOVA (f) or two-way ANOVA (g) with Holm-Sidak tests.

Table S3. Primers used in this study.

	Forward	Reverse
mHmox1	CAGAACCCAGTCTATGCCCC	GTGAGGCCCATACCAGAAGG
mNqo1	CTGCCATGTACGACAACGGT	ATCGGCCAGAGAATGACGTT
mGsta4	TTAATGGCAGGGGACGGATG	TACTTGGCCGAAAAGCAGGT
mDhrs9	AAGCTCGAGGGCGTGTTATC	ATTGAAACCCTCCACTGCGT
mSlc7a11	CAGGAGAAGGTAGTTCTGAAAAAGA	AGGGCTCCAAAAAGTGACAG
mAldh1l2	GGCTCCATCATCTACCACCC	CCAGAAAACAGAAAACCCAGCTT
mAU018091	TGCTGTGTTTCGTCTCCCTC	TGTACCACGGAGAATCCCCT
mSlc38a7	TGGCGCTCTTTATCCCTGAC	GGCTCCCAATGTGACCAGAA
mSlc3a2	TGAACGAGCTAGAACCGGAGA	CCTTGATCTTCACCAGACCGTT
mSlc7a5	GCTGACGAACCTGGCCTATT	ACCCATTGACAGAGCCGAAG
mSlc1a4	TGCTCTGGCGTTCATCATCA	AGACGTAGTGAATGCGGCAA
mSlc6a9	ATGTTCAAAGGCGTGGGCTA	GTGCGTCATGGACGAGAAGA
mSlc17a5	CTGCTCTGCTCGGTACAACT	CCGGGAATTGTGTGATTGTGG
mSlc7a3	CAGCACATTAGGTGCAGGTGT	TAACACAGTCCAGCCAACACA
mSlc6a8	CCCCTGTCATCGAGTTCTGG	AGGACCACGTAGGGGAATGT
mSlc7a1	GTTTCCCATGCCCCGAGTTA	AGTGGCGATTACGGGTGTTT
mSlc22a4	ACTCGGAACATTGCCACCAT	GCCAGAGAGGAAGCAGTTCA
mCtns	TATAGTGCCTCGCGGAGAGA	GGCAGGTCTGGTTGGAATGA
mCldn1	TTTGGCCAGGCCCTCTTTAC	AGGTTGTTTTCCGGGGACAG
mOcln	CTCGGTACAGCAGCAATGGT	CATAGTGGTCAGGGTCCGTC
mDsg3	AGTACCGAGTGCAGTCAACG	CCCGTGTCCTCATCAGTAGC
mDsg1a	TGGGGAATATAAAGGAACAGTGCT	CGTTGTGGGTTCTCAGTGGA
mDsg1b	TGGGGAATATAAAGGAACAGTGCTA	GTCACTGGGTCACGATTACCA
mK14	TGGTATCGGTGGTGGCTCTA	GAAGCGAGAGGAGGTAACCG
mK10	CAGTTCTCTTCCTCCCGCAG	GTAACCACCTGATGAGCCCC
hGLUT1	TGGCATCAACGCTGTCTTCT	CTAGCGCGATGGTCATGAGT
hGLUT2	GTGCTGGGTTCCTTCCAGTT	ACAGTCTCTTCCTCAGCCCA
hGLUT3	TGGGTCGCTTGGTTATTGGC	AGGAAGGATGGTAAAACCCAGT
hGLUT4	GTCTCGGTGTTGTTGGTGGA	TGGCCACAATGGAGACGTAG
hGLUT5	GTGCCCCAGCTCTTCATCAC	AGCGTCTGTAGGGCTTTCTTG
hGLUT6	CCATGCTCTTCATCATGGGCTA	GAAGGACTTGGTGAGGACGAA
hGLUT7	ACATCGCGGGACATTCCATT	GGCAGATTCCGGCAAAGATG
hGLUT8	CATCTGCGTCCTCACCAACT	GAAGATGCAGAAAGCGGAGG
hGLUT9	AGTGTGACCACCTGAGGAGT	AGCCGTAGAGGAAGGAGGAG
hGLUT10	ACCCTGTGGAGATACGAGGA	GCCGATGGTGCCAATGAGAT
hGLUT11	CCGGAAGCGAAGATCCAGTA	ACAGTGAAGATGCTCCCCCA
hGLUT12	AAGAGAGGGGAGACGACCTC	CATGGCTCGTCCTCTGATCC
hGLUT13	TGGCTTGTTGAGAAGGTGGG	CTTGTAGCAGAAACCGCAGTC
hSGLT1	TCGGACTGTGGGCTATGTTT	AGATGGGGACAAACAGCCAG
hSGLT2	CATCCCCAGAAAGCACCTCC	CCTGGGGCTCATTCATCTCC
h-β-actin	AAATCGTGCGTGACATTAAGGA	GCCATCTCTTGCTCGAAGTC
mGlut1	CTCACCACGCTTTGGTCTCT	CCCAGTTTGGAGAAGCCCAT
mGlut2	GCCCAGCAGTTCTCAGGAAT	ACATGCCAATCATCCCGGTT
mGlut3	CAGGTCACCCAACTACGTCC	TATGCAGGGTTCTCCTCCCT
mGlut4	GGATTCCATCCCACAAGGCA	CCAACACGGCCAAGACATTG
mGlut5	CGCGATCTACTACTACGCCG	CGTCAGCACTAAGCAGGCTA
mGlut6	AACAGAAGGGTGTTCCTGGC	AAGGTGAACACGGACCCAAA

mGlut7	AACAGATGGGGTCCTGTCTTTC	GTTCCCTTTCTGCCCCACTTA
mGlut8	TCTTCATTGCTGGCTTTGCG	TTGGTGAGGACACAGATGCC
mGlut9	CACCAGCAGAGGAGGACAAA	AGTCAGGGTATCCGGGTCAA
mGlut10	CGCCTCTACCATCTTTCGCT	TATGCCGCTGACCGATAAGG
mGlut12	TGCTGAACCAGAAGGGGAGA	CCCGATGAGGAGGGAACTCA
mGlut13	AGAAAGTGGGTCGCAGGAAG	AAAGTGACCCGTGGTGAGAC
mSGLT1	CCTGTGGTACTGGTGTACGG	CGATGTTGGTACAGCCCACT
mSGLT2	ATTGGTGTTGGCTTGTGGTC	AAAATGACCGCTGCCGATGT
m-β-actin	AAATCGTGCGTGACATCAAAGA	GCCATCTCCTGCTCGAAGTC
hPI3 (elafin)	AACACCTTCCTGACACCATG	CATTGAATGGAACACGGCC
hDEFB4	GACTCAGCTCCTGGTGAAGC	GGAGGGGAATGAGAGGAGAC
hS100A7	CCCAACTTCCTTAGTGCCTG	CTCTGCTTGTGGTAGTCTGTG
hS100A8	GTTCTGTTTTTCAGGTGGGGC	CAGGGAGTACTTGTGGTAGACG
hCXCL3	CCGAAGTCATAGCCACACTCAA	GTGCTCCCCTTGTTCAGTATCTT
hCCL3	ACCAGTTCTCTGCATCACTTGC	TGCTCGTCTCAAAGTAGTCAGC
mIFN γ	AAGACAATCAGGCCATCAGCA	ATGCATCCTTTTTCGCCTTGC
mIL-1β	TGAAATGCCACCTTTTGACAGTGAT	GGTTTGGAAGCAGCCCTTCAT
mS100A8	ACTTCGAGGAGTTCCTTGCG	TACTCCTTGTGGCTGTCTTTGT
mS100A9	CCTGGACACAAACCAGGACA	GTGGGTTGTTCTCATGCAGC
mCxcl3	CACCCTACCAAGGGTTGATTTTG	GTGGCTATGACTTCTGTCTGGG
mCcl3	ACCATGACACTCTGCAACCA	TCAACGATGAATTGGCGTGG
mTNFα	GACGTGGAACTGGCAGAAGAG	ACCGCCTGGAGTTCTGGAA
mIL-6	CCACGGCCTTCCCTACTTC	TTGGGAGTGGTATCCTCTGTGA